Phosphoric Metabolites Link Phosphate Import and Polysaccharide Biosynthesis for *Candida albicans* Cell Wall Maintenance

Ning-Ning Liu,[a*] Maikel Acosta-Zaldívar,[a] Wanjun Qi,[a] Joann Diray-Arce,[a,b] Louise A. Walker,[c] Theodore J. Kottom,[d] Rachel Kelly,[e] Min Yuan,[f,i] John M. Asara,[f,g] Jessica Ann Lasky-Su,[e] Ofer Levy,[a,b] Andrew H. Limper,[d] Neil A. R. Gow,[h*] Julia R. Köhler[a]

[a]Division of Infectious Diseases, Boston Children's Hospital/Harvard Medical School, Boston, Massachusetts, USA
[b]Precision Vaccines Program, Boston Children's Hospital, Boston, Massachusetts, USA
[c]Aberdeen Fungal Group, Institute of Medical Sciences, Medical Research Council Centre for Medical Mycology at the University of Aberdeen, Aberdeen, United Kingdom
[d]Thoracic Diseases Research Unit, Departments of Medicine and Biochemistry, Mayo Clinic College of Medicine, Rochester, Minnesota, USA
[e]Channing Division of Network Medicine, Brigham and Women's Hospital/Harvard Medical School, Boston, Massachusetts, USA
[f]Division of Signal Transduction, Beth Israel Deaconess Medical Center, Boston, Massachusetts, USA
[g]Department of Medicine, Harvard Medical School, Boston, Massachusetts, USA
[h]Medical Research Council Centre for Medical Mycology at the University of Aberdeen, Institute of Medical Sciences, Aberdeen, United Kingdom
[i]Mass Spectrometry Core, Beth Israel Deaconess Medical Center, Boston, Massachusetts, USA

Ning-Ning Liu, Maikel Acosta-Zaldívar, Wanjun Qi, and Joann Diray-Arce contributed equally. Author order was determined in order of seniority of participation in the corresponding author's group.

ABSTRACT The *Candida albicans* high-affinity phosphate transporter Pho84 is required for normal Target of Rapamycin (TOR) signaling, oxidative stress resistance, and virulence of this fungal pathogen. It also contributes to *C. albicans*' tolerance of two antifungal drug classes, polyenes and echinocandins. Echinocandins inhibit biosynthesis of a major cell wall component, beta-1,3-glucan. Cells lacking Pho84 were hypersensitive to other forms of cell wall stress beyond echinocandin exposure, while their cell wall integrity signaling response was weak. Metabolomics experiments showed that levels of phosphoric intermediates, including nucleotides like ATP and nucleotide sugars, were low in *pho84* mutant compared to wild-type cells recovering from phosphate starvation. Nonphosphoric precursors like nucleobases and nucleosides were elevated. Outer cell wall phosphomannan biosynthesis requires a nucleotide sugar, GDP-mannose. The nucleotide sugar UDP-glucose is the substrate of enzymes that synthesize two major structural cell wall polysaccharides, beta-1,3- and beta-1,6-glucan. Another nucleotide sugar, UDP-*N*-acetylglucosamine, is the substrate of chitin synthases which produce a stabilizing component of the intercellular septum and of lateral cell walls. Lack of Pho84 activity, and phosphate starvation, potentiated pharmacological or genetic perturbation of these enzymes. We posit that low substrate concentrations of beta-D-glucan- and chitin synthases, together with pharmacologic inhibition of their activity, diminish enzymatic reaction rates as well as the yield of their cell wall-stabilizing products. Phosphate import is not conserved between fungal and human cells, and humans do not synthesize beta-D-glucans or chitin. Hence, inhibiting these processes simultaneously could yield potent antifungal effects with low toxicity to humans.

IMPORTANCE *Candida* species cause hundreds of thousands of invasive infections with high mortality each year. Developing novel antifungal agents is challenging due to the many similarities between fungal and human cells. Maintaining phosphate balance is essential for all organisms but is achieved completely differently by

fungi and humans. A protein that imports phosphate into fungal cells, Pho84, is not present in humans and is required for normal cell wall stress resistance and cell wall integrity signaling in *C. albicans*. Nucleotide sugars, which are phosphate-containing building block molecules for construction of the cell wall, are diminished in cells lacking Pho84. Cell wall-constructing enzymes may be slowed by lack of these building blocks, in addition to being inhibited by drugs. Combined targeting of Pho84 and cell wall-constructing enzymes may provide a strategy for antifungal therapy by which two sequential steps of cell wall maintenance are blocked for greater potency.

KEYWORDS *Candida albicans*, Pho84, antifungal agents, cell wall, chitin synthase, glucan synthase, nucleotide sugar, phosphate metabolism

Candida species are the most commonly isolated invasive human fungal pathogens. Only 3 drug classes are currently available to treat invasive candidiasis, whose attributable mortality is estimated at 19 to 24% (1). Among them, echinocandins, inhibitors of the enzyme beta-1,3-glucan synthase that produces a major cell wall component of *Candida* species, are now recommended as first-line therapy, since they are candidacidal and have few adverse effects or drug interactions (2, 3). Still, outcomes of invasive candidiasis are often poor (2). In fact, early biochemical studies showed that enzymatic activity of beta-1,3-glucan synthase is inhibited by no more than 80% by the echinocandins (4), i.e., echinocandins do not completely inhibit their target (5). Potentiating their effect could be one strategy to improve outcomes in this fearsome infection.

A major barrier to development of new antifungal drugs is the high degree of conservation of many potential drug targets between fungi and humans. We recently found that genetic or pharmacologic interference with the activity of a *Candida albicans* cell surface phosphate (P_i) transporter, Pho84, which has no human homolog, can indirectly inhibit TOR complex 1 (TORC1) and thereby selectively target fungal proliferation (7). Loss of Pho84 activity also sensitizes *C. albicans* to oxidative stress and potentiates the activity of two antifungal agents, the polyene amphotericin B and the echinocandin micafungin (7, 8).

Micafungin inhibits *C. albicans* beta-1,3-glucan synthase (9). Questioning how Pho84 activity is related to this enzyme, we found that cells lacking *PHO84* poorly tolerated each cell wall stress that we examined. Responsiveness of their cell wall integrity (CWI) pathway signaling through Mkc1 was reduced compared to the congenic wild type. Unlike their oxidative stress hypersensitivity phenotypes (8), homozygous null mutants in *PHO84* ($pho84^{-/-}$) did not recover cell wall stress resistance by overexpression of the TORC1-activating GTPase, Gtr1. Hence, cell wall stress hypersensitivity of cells lacking Pho84 was mechanistically distinct from their susceptibility to oxidative stress.

Metabolomics experiments showed that cells lacking Pho84 contained significantly fewer nucleotides and nucleotide sugars than wild-type cells during recovery from P_i starvation. Two nucleotide sugars, UDP-glucose and UDP-*N*-acetylglucosamine (UDP-GlcNAc), whose levels in $pho84^{-/-}$ cells were decreased, are substrates of the enzymes that produce major cell wall polysaccharides. UDP-GlcNAc is the substrate for chitin synthases (6, 10–14). UDP-glucose is the substrate for beta-1,3-glucan synthases Fks1 and Fks2 (5), as well as for beta-1,6-glucan synthases Kre6 and Skn1 (15–18). We hypothesized that provision of P_i contributes to the availability of precursors for beta-D-glucan and chitin biosynthesis.

Our hypothesis predicts that cells lacking P_i or Pho84 activity are also hypersensitive to chemical or genetic perturbation of chitin synthase and beta-1,6-glucan synthase, in addition to beta-1,3-glucan synthase inhibition. We focused on the former two biosynthetic processes, since they may be amenable in the future to pharmacologic inhibition, while excellent beta-1,3-glucan synthase inhibitors are already clinically available or in development (19). Lack of Pho84, P_i starvation, genetic depletion of these enzymes, and pharmacologic inhibition of chitin synthase had combinatorial effects on *C. albicans*
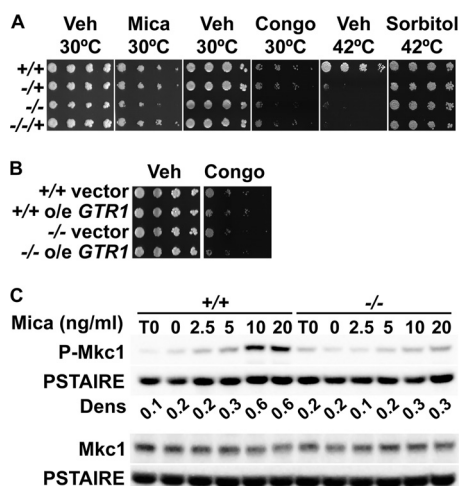
FIG 1 The role of Pho84 in cell wall stress resistance was not mediated by TORC1 but corresponded to weak cell wall integrity signaling. (A) Cell dilutions, shown horizontally, were spotted onto synthetic complete medium (SC) with 1 mM KH_2PO_4 with vehicle (Veh) and 25 ng/ml micafungin (Mica), yeast extract-peptone-dextrose (YPD) without or with 50 μg/ml Congo red (Congo), and YPD without or with 1 mM sorbitol and incubated at 30°C (micafungin and Congo red assay) or 42°C (heat resistance and osmotic rescue testing). Strains: +/+, *PHO84/PHO84*, JKC915; −/+, *pho84/PHO84*, JKC1583; −/−, *pho84/ pho84*, JKC1450; −/−/+, *pho84/pho84::PHO84*, JKC1588. (B) Wild-type (+/+) and *pho84* null mutant (−/−) cells with integrated empty overexpression vector (vector) or overexpressing (o/e) *GTR1* were spotted onto YPD medium with vehicle or 50 μg/ml Congo red (+/+ vector, JKC1594; +/+ o/e *GTR1*, JKC1596; −/− vector, JKC1598; −/− o/e *GTR1*, JKC1600). (C) Western blot analysis of wild-type (+/+, JKC915) and *pho84* null (−/−, JKC1450) cells grown for 90 min in SC with 0.2 mM KH_2PO_4 with increasing concentrations of micafungin, probed with antibody to phosphorylated Mkc1 (P-Mkc1), total Mkc1 (Mkc1), and the PSTAIRE antigen of Cdc28 as loading control. Dens, ratio of densitometry of P-Mkc1 to PSTAIRE signal intensity.

growth. Pharmacologic inhibition of Pho84 therefore might potentiate not only echinocandin antifungal activity but also that of other inhibitors of cell wall biosynthetic enzymes.

RESULTS

A Pho84 contribution to cell wall stress resistance was independent of TORC1. *C. albicans PHO84* mRNA levels are upregulated during the interaction with host cells as found by others in *ex vivo* models (20, 21) and *in vivo* during experimental infections (22, 23). Cells lacking Pho84 are attenuated in virulence (8). We tested the responses of mutants in *PHO84* to stresses they might encounter during infection. Having found that loss of Pho84 potentiates the activity of the echinocandin micafungin (7), we asked whether Pho84 has a role in tolerance of other cell wall stressors which do not act through beta-1,3-glucan synthase inhibition. Congo red is an anionic dye which is thought to disrupt fungal cell wall assembly by binding to the cell wall polysaccharide chitin and disrupting the enzymatic reactions that connect chitin to the glucans, thereby weakening the cell wall (24). Cells lacking Pho84 poorly tolerated chemical cell wall stress induced by Congo red exposure (24) and physical stress induced by heat exposure with osmotic rescue (25, 26) (Fig. 1A). These findings indicate that *pho84*$^{-/-}$ mutants are hypersensitive to cell wall stressors that act by diverse mechanisms.

We previously found an activating activity of Pho84 toward TORC1 to be required for rapamycin tolerance (7). Rapamycin hypersensitivity and Sod3 depletion phenotypes of *pho84*$^{-/-}$ cells can be suppressed by overexpression of *GTR1*, which encodes a GTPase component of the TORC1-activating EGO complex (7). *GTR1* overexpression had no effect on cell wall stress hypersensitivity of *pho84*$^{-/-}$ cells (Fig. 1B), suggesting that Pho84 is required for cell wall stress resistance independently of its TORC1-activating role.

Pho84 was required for cell wall integrity signaling. *C. albicans* cells experiencing cell wall stress induce the CWI signaling pathway (27), whose activity corresponds to
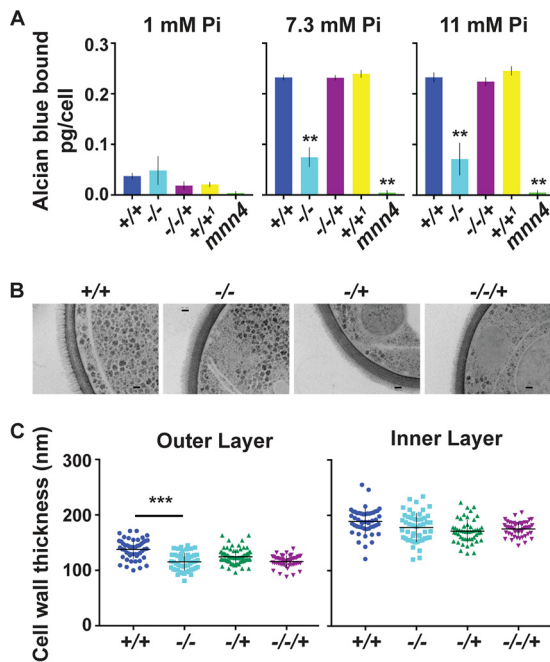
FIG 2 Pho84 was required for a normal phosphomannan cell wall layer. (A) Alcian blue staining. Cells were grown in SC with 1 mM, 7.3 mM, or 11 mM P_i for 15 h, and alcian blue staining was assayed in 3 technical replicates. Strains: $+/+$, PHO84/PHO84, JKC915; $-/-$, pho84/pho84, JKC1450; $-/-/+$, pho84/pho84::PHO84, JKC1588; $+/+^1$, PHO84/PHO84 CAI-4/CIp10; mnn4, mnn4::hisG-URA3-hisG/mnn4::hisG, CDH5. Representative of 3 biological replicates. (B) Transmission electron micrographs of wild-type ($+/+$, JKC915), pho84 null mutant ($-/-$, JKC1450), pho84 heterozygote ($-/+$, JKC1583), or PHO84 reintegrant ($-/-/+$, JKC1588) cells. Bar, 100 nm. (C) Thickness measurements of outer and inner cell wall layer of cells ($n = 50$) imaged as in panel B. Error bars show standard deviations (SD).

the phosphorylation state of its mitogen-activated protein (MAP) kinase, Mkc1 (28). Mkc1 phosphorylation in response to micafungin was weak in cells lacking Pho84 in P_i-poor medium (Fig. 1C), indicating defective activation of CWI signaling. Decreased Mkc1 phosphorylation was less pronounced but still detectable in rich complex medium yeast extract-peptone-dextrose (YPD), which contains 2 mM inorganic phosphate (P_i) as well as accessible organic phosphate compounds (29) (see Fig. S1 in the supplemental material), suggesting that lack of Pho84 impacts CWI signaling even in environments of higher P_i abundance. C. albicans TORC1 inhibition is known to upregulate Mkc1 phosphorylation (30), so increased sensitivity of pho84$^{-/-}$ mutants to cell wall stress and their decreased CWI signaling are apparently due to a TORC1-independent mechanism.

Cell walls of pho84$^{-/-}$ mutants showed decreased alcian blue staining, consistent with decreased cell wall phosphomannan. A major component of C. albicans cell walls is phosphomannan. Phosphodiesters link oligomannosides to glycosylated proteins on the cell surface (31), forming a fibrillar outer layer exterior to the strong chitin and glucan mesh that forms the structural inner layer of the cell wall (32). The phosphomannan component of the C. albicans cell wall confers a negative charge, which can be quantified by binding of the cationic dye alcian blue (33, 34). We questioned whether cells confronting a limiting P_i supply might prioritize its use for essential metabolic processes over cell wall construction. Using control cells deleted for MNN4, which lack phosphomannan (34), we found decreased alcian blue staining of pho84$^{-/-}$ cell walls during growth at replete (7.3 mM, the concentration of standard synthetic complete medium [SC]) and excess (11 mM) P_i concentrations. At moderate P_i concentrations (1 mM), the wild type also produced less cell wall phosphomannan, and the difference between pho84$^{-/-}$ and wild-type cells was within the sensitivity range of the assay (Fig. 2A). In transmission electron microscopic (TEM) images, the outer cell wall layer of pho84$^{-/-}$ as well as pho84$^{-/+}$ and pho84$^{-/-/+}$ mutant cells was thinner

than that of wild-type cells (Fig. 2B and C), suggesting that these cells' diminished phosphomannan measurably perturbs the cell wall architecture.

Pho84 was required for production of cell wall polymer precursors. Mannosylation of proteins and addition of phosphomannan occur in the Golgi apparatus where GDP-mannose is the sugar donor (31). The importance of GDP-mannose availability is evinced by the finding that transport of GDP-mannose into the Golgi lumen is the rate-limiting step in cell surface protein mannosylation (31). More generally, nucleotide sugars are precursors of cell wall polymers, e.g., UDP-glucose for beta-1,6- and beta-1,3-glucan (5, 16) and UDP-GlcNAc for chitin (35). To examine whether loss of Pho84 affects the availability of biosynthetic intermediates required for cell wall production, we compared metabolomes of wild-type and $pho84^{-/-}$ cells recovering for 4 h in synthetic complete medium (SC) with low (0.22 mM) or excess (11 mM) KH_2PO_4 from P_i starvation, induced by 3 days' incubation in SC medium without P_i (SC-P_i) as in the work of Popova et al. (36). This pregrowth period was important in order to unmask P_i starvation effects that are otherwise buffered by vacuolar polyphosphate stores in *Saccharomyces cerevisiae* (37) and are predicted to act similarly in *C. albicans* (38). Cells grown in this manner, washed in sterile water three times, were extracted three times in 80% methanol for 40 min at −80°C; supernatants were pooled and dried in a SpeedVac and then stored at −80°C until analysis.

Hydrophilic interaction liquid chromatography-mass spectrometry (LC-MS/MS) was performed as described in reference 39 to quantitate 258 known metabolites, comparing $pho84^{-/-}$ cells with wild type. We identified significantly altered compounds and pathways using MetaboAnalyst (40). Principal-component analysis showed clustering of genotypes and of ambient P_i availability (Fig. 3A). High reproducibility between experiments and significant differences between wild-type and $pho84^{-/-}$ cells were observed by arraying the metabolites measured in three biological replicates (from cells grown on different days) in a heat map (Fig. 3B). The heat map illustrates data values scaled by metabolite abundance in arbitrary units across treatments for each metabolite feature. Similarity measure is based on Euclidean distance and clustered using Ward's linkage.

The genotypes, $pho84^{-/-}$ mutant and wild type, clustered together primarily (Fig. 3B). Low and excess P_i concentrations between the two genotypes did not cluster. Closer inspection showed that within some clusters of metabolites, highlighted by rectangles in Fig. 3B, the relative intensities of metabolites were more similar among $pho84^{-/-}$ cells in low P_i and wild type in excess P_i and vice versa than among similar ambient P_i concentrations between the two genotypes. Possibly, some metabolic alterations in cells without Pho84 activity may not be due just to lack of P_i but also to aberrant regulatory responses.

Biological process enrichment analysis revealed pyrimidine biosynthesis as among the most significantly affected metabolic pathways during growth of $pho84^{-/-}$ mutant cells at both low and excess ambient P_i (Fig. 3C). Purine biosynthesis was also highly significantly altered, as was nucleotide sugar metabolism. We concluded that loss of Pho84 disturbs metabolism of compounds required in cell wall polymer biosynthesis.

Among individual metabolites, purine and pyrimidine nucleotide levels were decreased in $pho84^{-/-}$ cells compared with wild type, while the bases uracil and cytosine and the nucleosides cytidine and guanosine were substantially increased in $pho84^{-/-}$ cells (see Table S1 in the supplemental material). For nucleotide products derived from each nucleobase, we observed accumulation of metabolites before a phosphorylation step and their depletion after this step (Fig. 3D). The most important phosphoric nucleotide precursor, phosphoribosyl-pyrophosphate (PRPP), was sharply decreased (Fig. 3E). These results were obtained using MetaboAnalyst; the column-wise means of all samples from *pho84* null mutant cells were divided by the column-wise means of all samples from wild-type cells before column normalization; absolute value changes were compared as fold change. The constellation of metabolic intermediates that we observed suggested that lack of nucleotides was due to a dearth of P_i, since interme-
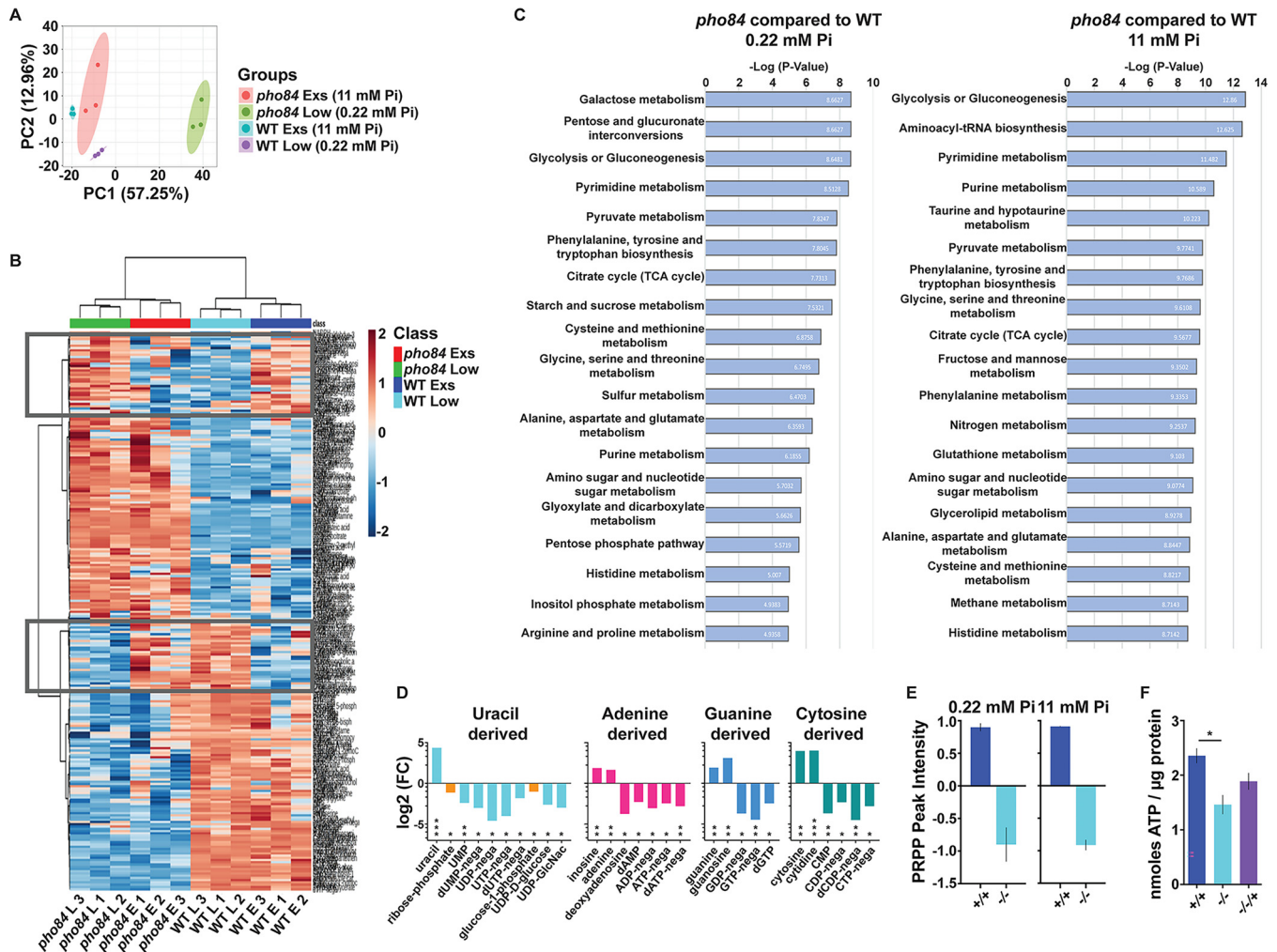
FIG 3 LC-MS/MS measurements of metabolites showed clustering of wild-type versus *pho84* null mutant cells and reflected perturbation of metabolic pathways that contain phosphorylation steps. Cells of the wild type (+/+, JKC915) or *pho84* null mutant (−/−, JKC1450) were grown in SC-P$_i$ for 3 days and then fed for 4 h with low (0.22 mM) or excess (11 mM) KH$_2$PO$_4$ in SC. Cell extracts were subjected to LC-MS/MS for untargeted global metabolomics. (A) Multivariate principal-component analysis shows clustering of profiles according to sample grouping. (B) Unsupervised hierarchical clustering using Euclidean distance of 3 biological replicates for each sample condition (wild type or *pho84* null mutant, low or excess P$_i$); red-to-blue scale represents high to low metabolite levels. (C) Summary plot of metabolite set enrichment analysis; significant metabolite groups are ranked according to negative log *P* value. TCA, tricarboxylic acid. (D) Metabolite abundance within biosynthetic pathways of nucleotides and nucleotide sugars, shown as log$_2$ of fractional relative intensities of each metabolite in *pho84* null mutant cells versus wild-type cells. ***, *P* (adjusted) < 0.0001; **, *P* (adjusted) = 0.0001 to 0.001; *, *P* (adjusted) = 0.001 to 0.05. (E) Relative abundance of phosphoribosyl-pyrophosphate (PRPP) in *pho84* null mutant (−/−, JKC1450) versus wild-type (+/+, JKC915) cells grown in the stated concentrations of KH$_2$PO$_4$, shown as scaled, normalized LC-MS/MS peak intensity. (F) ATP concentrations of wild-type (+/+, JKC915), *pho84* null mutant (−/−, JKC1450), or reintegrant (−/−/+, JKC1588) cells grown in rich medium (YPD) for 15 h, expressed as nmol ATP/μg protein. *, *P* = 0.002. Representative of 3 biological replicates.

diates destined for phosphorylation seemed to have accumulated upstream of the cognate kinase. Degradation products of purines like allantoin were strongly decreased, suggesting that purine salvage was highly upregulated (Table S1).

To test the apparent lack of nucleotides independently, we measured the concentration of the most important nucleotide, ATP, in cells grown to saturation in rich complex medium as in the work of Grahl et al. (41). *pho84*$^{-/-}$ cells contained substantially less ATP than wild-type or −/−/+ *PHO84* reintegrant cells (Fig. 3F), confirming the result of the LC-MS/MS experiments. Metabolic derangements of *pho84*$^{-/-}$ cells were extensive and involved multiple further biosynthetic pathways (Fig. 3C and Table S1). Since ATP participates in a majority of metabolic processes (42), its decreased availability could drive many of the metabolic effects that we observed.

Loss of Pho84 decreased the amount of detectable cell wall chitin. UDP-GlcNAc, the substrate of chitin synthases, was the most significantly decreased cell wall pre-
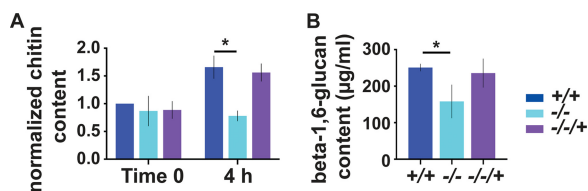
FIG 4 Pho84 activity contributed to cell wall chitin and beta-1,6-glucan synthesis. (A) Chitin content of cells of indicated *PHO84* genotypes. Chitin staining with calcofluor white was quantified by flow cytometry of $\geq 10^5$ events; fluorescence intensity signals were normalized using the wild-type time zero readings for each of 3 biological replicates whose combined results are shown. (B) Alkali-insoluble beta-1,6-glucan content of cells grown as in panel A was measured by ELISA. Error bars show SD for 3 biological replicates. *, $P < 0.05$. +/+, wild type, JKC915; −/−, *pho84* null mutant, JKC1450; −/−/+, *PHO84* reintegrant, JKC1588.

cursor requiring a pyrimidine in *pho84*$^{-/-}$ cells (Table S1). We hypothesized that if P_i to produce specific pyrimidine nucleotide sugars is insufficient, the cell wall polymers produced from these nucleotide sugars will be diminished. To measure cells' chitin content, we modified an assay described in reference 43, using wild-type cells with decreased chitin content for validation. Cells were grown overnight in SC with 0.5 mM P_i, unexposed or exposed to increasing concentrations of the chitin synthase inhibitor nikkomycin Z (nikkomycin) (Fig. S2A) (44, 45), a competitive inhibitor of *C. albicans* chitin synthases (44). Fluorescence intensity of calcofluor white-stained cells, recorded by flow cytometry, clearly reflected the decreased chitin content and dose response of nikkomycin-exposed cells (Fig. S2A).

We then measured the chitin content in wild type, *pho84*$^{-/-}$ mutant, and −/−/+ *PHO84* reintegrant cells recovering from P_i starvation, as in the metabolomics experiments, during growth in SC with low (0.22 mM) P_i for 4 h. Cells without Pho84 had a significantly lower chitin cell wall content than wild-type and reintegrant cells (Fig. 4A and Fig. S2B). Chitin quantitation results were highly numerically reproducible among biological replicates performed on different days (Fig. 4A), when measurements were normalized to the mean fluorescence of wild-type cells harvested at the end of P_i starvation (time zero). This result suggests a robust metabolic or signaling-based regulatory system that directs biosynthetic fluxes in P_i-starved *pho84*$^{-/-}$ cells away from chitin production and provides a possible causal link to the role of Pho84 in cell wall stress resistance.

Less beta-1,6-glucan was detected in *pho84*$^{-/-}$ cell walls. In *Saccharomyces cerevisiae*, abundant covalent linkages of beta-1,6-glucan to 3 other cell wall components, beta-1,3-glucan, chitin, and mannoproteins, suggested a critical structural function of beta-1,6-glucan as the central "glue" for the distinct polymers that make up the cell wall (46). Beta-1,6-glucan, comprising >50% of alkali-insoluble cell wall glucan in *C. albicans* (16), is produced by two conserved homologous synthases, Kre6 and Skn1 (16, 18), whose *S. cerevisiae* homologs utilize UDP-glucose as the substrate (15, 47). An enzyme-linked immunosorbent assay (ELISA) used in *Pneumocystis carinii* (48) was adapted to compare the beta-1,6-glucan contents of wild-type and *pho84*$^{-/-}$ cells recovering from P_i starvation; a strain in which *KRE6* transcription was repressible from the *MAL2* promoter (pMAL2) served as the control in establishing the assay (Fig. S3A).

Fungal cell wall components are classically analyzed from 2 fractions, alkali insoluble and soluble; the major alkali-insoluble fraction represents a mesh of chitin fibrils covalently linked to glucans (49, 50) which provides the structural stability and shape to the cell wall (51). In *S. cerevisiae*, the covalent bond lending insolubility, in hot NaOH, to this cell wall fraction consists of chitin linked to the nonreducing end of a beta-1,3-glucan chain (52). We quantified beta-1,6-glucan in alkali-insoluble cell wall fractions. Alkali-insoluble cell wall fractions from *pho84*$^{-/-}$ cells contained significantly less beta-1,6-glucan than those from wild-type cells (Fig. 4B). Additionally, we examined alkali-soluble fractions. The alkali-soluble cell wall fraction of *C. albicans* comprises 5 to 11% of the cell wall mass depending on growth conditions (53) and represents glucans

unlinked to the chitin-glucan mesh that forms the mechanoresistant cell wall core. The alkali-soluble cell wall fraction of $pho84^{-/-}$ mutant cells contained more beta-1,6-glucan than that of the wild type (Fig. S3B), suggesting a reduction in covalent linkages among the major cell wall polysaccharides in these cells; the reduction in cell wall chitin content (Fig. 4A and Fig. S2B) may be responsible for this finding. Overall, major cell wall structural polysaccharides were diminished in cells lacking Pho84 activity, apparently paralleling the availability of their metabolic precursors.

Phosphate deprivation sensitized wild-type cells to pharmacologic inhibition of beta-1,3-glucan and chitin synthesis. If $pho84^{-/-}$ cells are hypersensitive to beta-1,3-glucan synthase inhibition because they lack P_i for production of precursors, depriving wild-type cells of P_i should have a similar effect. Activity of cell wall polysaccharide-synthetic enzymes decreases when they bind a specific inhibitor (4). By mass action, accumulation of their product should diminish further with declining concentrations of their substrates, i.e., when UDP-glucose and UDP-GlcNAc concentrations drop. Micafungin was used to inhibit beta-1,3-glucan synthase, and nikkomycin was used to inhibit chitin synthase. We had no pharmacological inhibitor of beta-1,6-glucan synthase since the only published such compound (54) is no longer available.

We questioned wild-type cells' responses under conditions that physiologically diminish the role of Pho84, using conditions where its expression in wild-type cells is low. We first established the highest P_i concentration at which *C. albicans* derepresses *PHO84* transcription, expecting that, as in *S. cerevisiae, PHO84* is repressed in high ambient P_i concentrations (37). Using a *PHO84* promoter-green fluorescent protein (GFP) fusion, we determined that the *PHO84* promoter became derepressed at ≤0.4 mM ambient P_i (Fig. S4); hence, we used 0.5 mM as a moderate P_i concentration during refeeding of P_i-starved cells. Wild-type cells starved for P_i in the same way as for the metabolomics experiments, or prefed with excess (12 mM) P_i, were reinoculated into moderate (0.5 mM) or excess (12 mM) P_i concentrations and exposed to inhibitors of beta-1,3-glucan- and of chitin synthesis. Cells were incubated in 2× SC with 2% glucose in these experiments, in order to optimize nutrients during inhibitor exposure.

Wild type cells prestarved for P_i before, and refed moderate P_i during, exposure to micafungin were significantly more sensitive than control cells provided with excess P_i throughout the experiment (Fig. 5A). However, P_i starvation during micafungin exposure did not lead to growth defects of a micafungin-resistant *C. albicans* bloodstream isolate from a patient treated long-term with this drug (Fig. 5B). This finding indicates that P_i starvation did not cause global growth defects in these experiments; it potentiated the effect of specific inhibitors of enzymes whose substrates are linked to P_i availability.

Growth defects induced by nikkomycin exposure were enhanced in cells prestarved for P_i and refed with moderate P_i (Fig. 5C), in wild-type cells as well as in the micafungin-resistant bloodstream isolate (Fig. 5D). Hence, P_i starvation sensitized wild-type cells to inhibition of two distinct sugar nucleotide-consuming cell wall biosynthetic processes.

Loss of Pho84 and P_i starvation sensitized cells to genetic depletion of chitin and beta-1,6-glucan synthases. If $pho84^{-/-}$ cells' hypersensitivity to cell wall stressors is due to insufficient concentrations of nucleotide sugars, cells with diminished activity of chitin and beta-1,6-glucan synthases should be hypersensitive to loss of Pho84 and to P_i starvation. To further test this idea, we perturbed these enzymes genetically.

Among the 4 chitin synthases of *C. albicans*, the only essential isoenzyme, Chs1, is required for septum production during cell division and contributes to the stability of lateral cell walls (55). We constructed mutants whose only *CHS1* allele is controlled by *pMAL2* or by *tetO*, repressible by glucose or doxycycline, respectively, and confirmed that they exhibit previously described phenotypes (13, 55) (Fig. S5). The effect of P_i availability during *CHS1* depletion was examined. *CHS1* was depleted from *pMAL2* or from *tetO* after a day of P_i starvation or P_i excess feeding during which *CHS1* expression
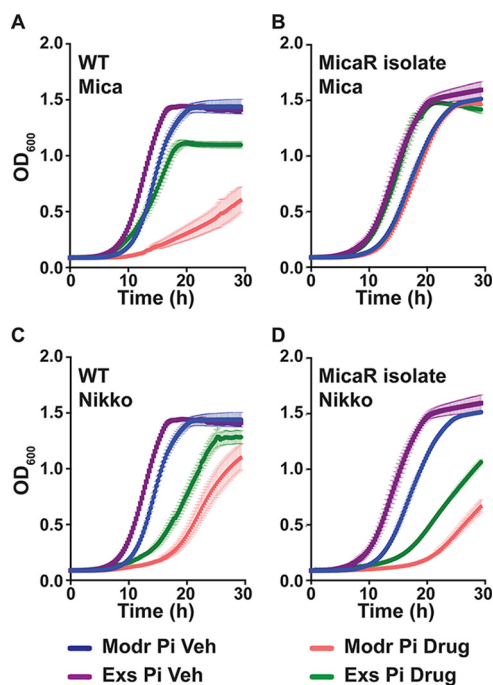
FIG 5 P_i starvation sensitized wild-type cells to inhibitors of two cell wall polysaccharide synthetic enzymes. (A and B) Growth of cultures exposed to vehicle or 40 ng/ml micafungin of the wild type (JKC915) or a micafungin-resistant bloodstream isolate (MicaR, JKC2490), pregrown in 2× SC without or with excess P_i for 1 day and inoculated into 2× SC with moderate (Modr) or excess (Exs) P_i, respectively. (C and D) Growth of cells exposed to vehicle or 8 μM nikkomycin of the wild type (JKC915) or a micafungin-resistant bloodstream isolate (JKC2490) treated as in panels A and B. Modr P_i, pregrown in 0 P_i, inoculated to 0.5 mM P_i with vehicle or drug; Exs P_i, pregrown with 12 mM P_i, inoculated to 12 mM P_i with vehicle or drug. Representative of 3 biological replicates; error bars show SD for 3 technical replicates.

was induced from these promoters, by incubation in maltose or in the absence of doxycycline. *CHS1*-depleted cells, incubated in glucose or doxycycline, respectively, had a significant growth defect in a moderate P_i concentration (0.5 mM) (Fig. 6A and B and Fig. S6). The specificity of the P_i-dependent growth defect of *CHS1*-depleted cells was demonstrated by comparatively robust growth of these cells fed excess P_i (Fig. 6A and B).

The role of Pho84 in cells depleted for *CHS1* was probed. Loss of *PHO84* potentiated the growth defects of cells depleted of *CHS1* even in cells fed excess P_i (Fig. 6A and B). These experiments suggest that as Chs1 activity became limiting because of a decline of its cognate transcript, P_i availability impacted growth significantly. Additionally, a Pho84-specific role seemed to emerge that was independent of ambient P_i concentrations.

We constructed strains in which a single allele of the gene encoding the major beta-1,6-glucan synthase, *KRE6* (16, 18), is controlled by *pMAL2*. Additionally, the gene encoding the second known beta-1,6-glucan synthase, *SKN1*, was deleted in the *kre6/pMAL2-KRE6* background (18). We observed more severe growth and filamentation phenotypes than did Han et al. (18) during exposure of 2 independent *kre6/KRE6* heterozygous deletion mutants to calcofluor white (Fig. 7A and B), and during depletion of *KRE6* from *pMAL2* in glucose. To reexamine our findings in light of these discordant results, we constructed strains in which a single *KRE6* allele is transcribed from repressible *tetO*. While neither of these repressible promoters can completely shut off transcriptional activity (56), the phenotypes we observed during repression of *KRE6* transcription from either promoter were inconsistent with those of Han et al.; phenotypes of 2 independently constructed lineages from 2 *kre6/KRE6* heterozygous strains were indistinguishable. In contrast to the findings of Han et al. (18), additional deletion
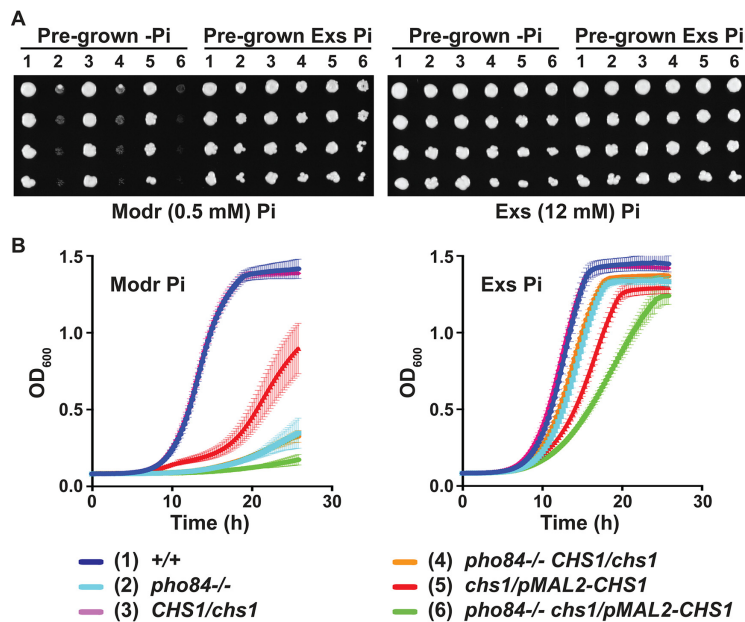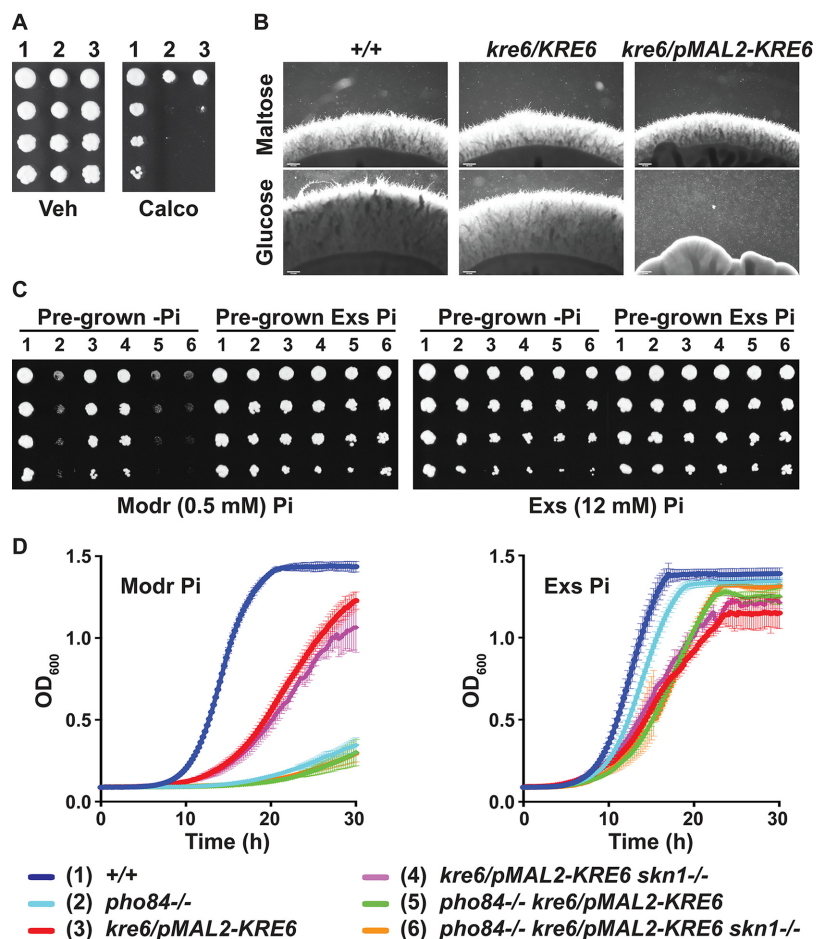
FIG 6 Growth defects of cells depleted of *CHS1* were potentiated by lack of Pho84 activity. (A) Cells of indicated genotypes were pregrown in 2× SC-2% maltose without or with excess P_i for 1 day, and dilutions were spotted on 2× SC-2% glucose medium containing moderate or excess P_i. Dilutions are shown vertically. (B) Cells pregrown without or with excess P_i as described in panel A were inoculated into 2× SC-2% glucose containing moderate or excess P_i, respectively. Representative of 3 biological replicates; error bars show SD for 3 technical replicates. +/+, JKC915; *pho84−/−*, JKC1450; *chs1/CHS1*, JKC2128; *pho84−/− chs1/CHS1*, JKC2141; *chs1/pMAL2-CHS1*, JKC2216; *pho84−/− chs1/pMAL2-CHS1*, JKC2235.

of *SKN1* contributed little to growth defects of *KRE6*-depleted cells under these experimental conditions (Fig. 7C and D).

To examine the effect of P_i availability on cells with decreased beta-1,6-glucan synthase activity, cells were P_i starved as for the metabolomics experiments but in 2× SC to allow for maximal growth and recovered in moderate (0.5 mM) or excess (12 mM) P_i. Control cells were P_i loaded in 12 mM P_i. Cells depleted for *KRE6* after P_i starvation and during recovery in moderate P_i concentrations had more severe growth defects than cells that were continuously fed excess P_i (Fig. 7C and D). This result suggested a need for P_i when levels of beta-1,6-glucan synthase became limiting, in order to supply sufficient concentrations of the enzyme's substrate, UDP-glucose.

Loss of Pho84 prevented compensatory chitin deposition in cells depleted for beta-1,6-glucan. Inhibiting beta-1,3-glucan synthesis pharmacologically with echinocandins or depleting beta-1,6-glucan synthases genetically induces compensatory synthesis of chitin by both transcriptional and posttranscriptional mechanisms (57–59). We measured chitin content of cells with and without *PHO84,* which were depleted for *KRE6* with or without intact *SKN1* loci (*kre6/pMAL2-KRE6* and *kre6/pMAL2-KRE6 skn1/skn1,* as well as *pho84/pho84 kre6/pMAL2-KRE6* and *pho84/pho84 kre6/pMAL2-KRE6 skn1/skn1*). Cells were precultured as for metabolomics experiments, except that maltose was provided as the carbon source to permit expression of *KRE6,* and 2× SC was used to allow for maximal provision of nutrients other than P_i. They were then grown for 8 h in 2× SC with 0.22 or 11 mM P_i as in metabolomics experiments, using glucose as the carbon source to repress *KRE6*.

We found a higher chitin content in cells depleted of *KRE6,* as previously reported (59). This effect was completely or partially abrogated in cells lacking Pho84 (Fig. 8A), depending on the ambient P_i concentration. Presence or absence of *SKN1* had no effect (Fig. 8A). We concluded that compensatory chitin synthesis in cells whose beta-1,6-glucan biosynthesis was diminished required the availability of sufficient P_i, as well as an activity of Pho84.

FIG 7 *KRE6* depletion resulted in filamentation defects and in growth defects potentiated by lack of Pho84 activity. (A) Wild-type cells (1, JKC915) and independent heterozygotes *kre6/KRE6* (2, JKC2111; 3, JKC2113) were spotted on YPD medium with vehicle or 30 μg/ml calcofluor white. (B) Filamentation of wild-type (+/+, JKC915), *kre6/KRE6* (JKC2111), and *kre6/pMAL2-KRE6* (JKC2204) cells on RPMI agar medium (pH 5.5) with 1.8% maltose and 0.2% glucose or 2% glucose, for 7 days at 37°C. Bar, 200 μm. (C) Cells of indicated genotypes (see bottom of figure) were pregrown in 2× SC-2% maltose without or with excess (12 mM) P_i for 3 days, and dilutions were spotted on 2× SC-2% glucose containing moderate (0.5 mM) or excess P_i. (D) Cells pregrown without or with excess P_i as in panel C were inoculated into 2× SC-2% glucose containing moderate or excess P_i, respectively. Representative of 3 biological replicates; error bars show SD for 3 technical replicates. +/+, JKC915; *pho84^{-/-}*, JKC1450; *kre6/pMAL2-KRE6*, JKC2204; *kre6/pMAL2-KRE6 skn1^{-/-}*, JKC2389; *pho84^{-/-} kre6/pMAL2-KRE6*, JKC2464; *pho84^{-/-} kre6/pMAL2-KRE6 skn1^{-/-}*, JKC2468.

Loss of Pho84 and chitin synthase inhibition potentiated growth defects during beta-1,6-glucan synthase depletion. When beta-1,3-glucan synthase is inhibited by an echinocandin, upregulation of chitin synthesis can compensate for loss of cell wall stability and inhibition of growth (57). We examined the effects of blocking compensatory mechanisms for loss of beta-1,6-glucan. Beta-1,6-glucan synthase was depleted by repressing *KRE6* from *pMAL2*, and Pho84 activity was eliminated genetically, while chitin synthase was inhibited with low concentrations of nikkomycin. Loss of Pho84 activity and chitin synthase inhibition each further reduced growth of cells lacking beta-1,6-glucan synthase (Fig. 8B). We concluded that the inhibitory effects of beta-1,6-glucan synthase depletion are potentiated by inhibition of chitin synthase and loss of Pho84 activity.

DISCUSSION

Cells lacking Pho84 are hypersensitive to cell wall stress (7) (Fig.1A). Our mechanistic analysis of this phenotype indicated that, unlike their oxidative stress hypersensitivity,
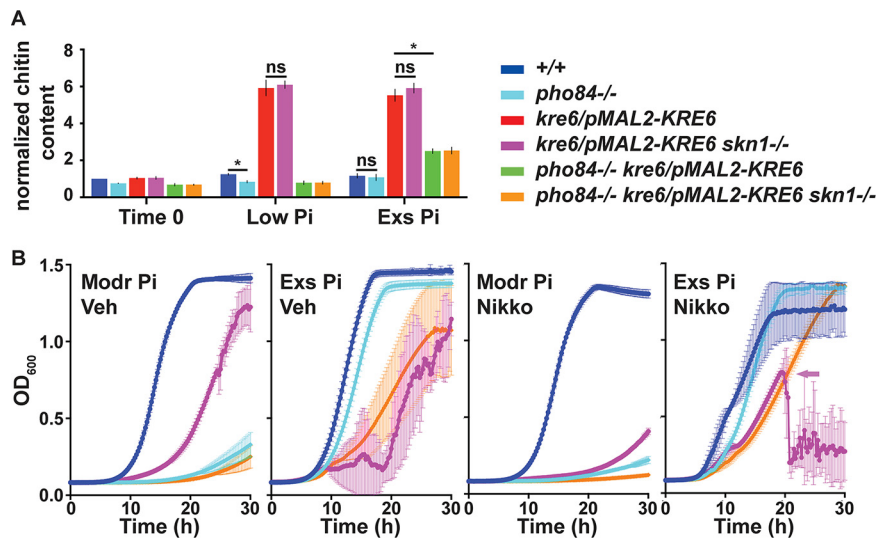
FIG 8 During *KRE6* depletion, Pho84 contributed to compensatory chitin synthesis and growth. (A) Cellular chitin content. After 3 days' passages in 2× SC-P$_i$-2% maltose (time zero), cells were grown for 8 h in 2× SC-2% glucose with low (0.22 mM) or excess (11 mM) P$_i$. Fluorescence intensity of calcofluor white-stained cells was measured by flow cytometry and normalized to wild-type time zero readings for each biological replicate. Error bars show SD for 3 biological replicates. *, $P < 0.05$; ns, not significant. (B) Growth during *KRE6* depletion, loss of Pho84, and chitin synthase inhibition. After 3 days' passages in 2× SC-2% maltose without or with excess P$_i$, cells were inoculated into 2× SC-2% glucose with moderate or excess P$_i$, respectively, with vehicle (Veh) or 0.25 μM nikkomycin (Nikko). Modr P$_i$, pregrown without P$_i$, inoculated to moderate (0.5 mM) P$_i$; Exs P$_i$, pregrown with excess (12 mM) P$_i$, inoculated to excess P$_i$. Representative of 3 biological replicates; error bars show SD for 3 technical replicates. +/+, JKC915; *pho84⁻/⁻*, JKC1450; *kre6/pMAL2-KRE6*, JKC2204; *kre6/pMAL2-KRE6 skn1⁻/⁻*, JKC2389; *pho84⁻/⁻ kre6/pMAL2-KRE6*, JKC2464; *pho84⁻/⁻ kre6/pMAL2-KRE6 skn1⁻/⁻*, JKC2468. Arrow in last panel of panel B indicates onset of overwhelming filamentation, at which time OD$_{600}$ ceased to reflect the cell number.

it was not directly related to these cells' diminished TORC1 signaling (Fig. 1B). While oxidative stress signaling is upregulated in *pho84⁻/⁻* cells (8), their cell wall integrity signaling was abnormally weak as measured by the phosphorylation state of the CWI MAP kinase Mkc1 (Fig. 1C). Dampened CWI signaling in *pho84⁻/⁻* cells cannot be explained by their decreased TORC1 signaling activity, because TORC1 inhibition induces signaling through Mkc1 (30). Decreased alcian blue staining of *pho84⁻/⁻* mutants suggested that the phosphomannoprotein content of their cell walls was decreased (Fig. 2A). Significant thinning of their outer phosphomannan cell wall layer was found by measurements of TEM images (Fig. 2B and C). This thinning was far less striking than that seen in TEM micrographs of mutants in enzymes that produce this layer, e.g., in the Mnn2 family of mannosyltransferases (60). Nevertheless, the difference in outer layer thickness between wild-type and *pho84⁻/⁻* cells was highly significant (Fig. 2C). The phenotype was similar in cells lacking one or both copies of *PHO84*. We noted striking haploinsufficiency of *pho84/PHO84* cells (and of *pho84/pho84::PHO84* cells) for outer cell wall layer thickness; haploinsufficiency is known to affect both structural and regulatory genes in *C. albicans* (61, 62). We concluded that lack of Pho84 can disturb the normal cell wall architecture.

This finding prompted the idea that cells lacking Pho84 are defective in synthesizing cell wall components that require phosphorylated precursors. Structural cell wall polysaccharides of *C. albicans*, beta-1,6-glucan, beta-1,3-glucan, and chitin in order of their abundance (16), are synthesized from monosaccharide precursors activated with UTP to generate UDP-containing nucleotide sugars; UTP biosynthesis requires availability of the P$_i$ donor ATP. Vacuolar polyphosphate stores buffer decreased extracellular P$_i$ availability in *S. cerevisiae* (37); vacuolar polyphosphate storage pools are also present in *C. albicans* (38). Hence, we applied the protocol of Popova et al. (36) to neutralize intracellular P$_i$ stores before an incubation period in low, moderate, or excess

P_i. Metabolomics experiments showed derangements of biosynthetic pathways that require phosphorylation steps in $pho84^{-/-}$ cells (Fig. 3). Pyrimidine biosynthesis was highly significantly altered. The sugar nucleotides that act as precursors for cell wall polysaccharide biosynthesis, UDP-glucose and UDP-GlcNAc, were decreased 2.6- and 2.9-fold, respectively, in $pho84^{-/-}$ cells in our experiments (Table S1). Our findings agree with those of Boer et al., who found decreased levels of nucleotides and of the nucleotide sugar UDP-glucose in P_i-limited *S. cerevisiae* cells grown in continuous culture in a chemostat (63).

We considered whether accumulation of toxic metabolites might account for cell wall biosynthesis defects. However, toxic metabolites that accumulate, e.g., in *S. cerevisiae* models of galactosemia (64, 65) and fructose intolerance (65), are sugar phosphates, i.e., their biosynthesis requires a phosphorylation step whose substrate was scarce in cells lacking Pho84. Accordingly, we did not identify potentially toxic metabolites among the significantly dysregulated metabolites in these cells (Table S1).

Perturbation of multiple other metabolic processes was observed. This result is consistent with depletion of ATP, a major P_i donor and energy currency of the cell, which we confirmed in independent assays for $pho84^{-/-}$ cells (Fig. 3F). Glycolysis and galactose and pentose processing were disrupted (Fig. 3C), consistent with a requirement for phosphorylation in metabolism of these sugars; glycolysis alone consumes 2 P_i and 2 ADP molecules per molecule of glucose (66). Possibly, defects in producing sugar precursors of nucleotide sugars may contribute to the disruption of nucleotide biosynthesis that we observed in cells lacking Pho84. Insufficient ATP to produce nucleotide sugars may also be ultimately responsible for cell wall phenotypes of cells perturbed in mitochondrial function, as reported, e.g., in references 67 to 72. However, ATP deprivation is expected to impact $pho84^{-/-}$ cells' fitness in multiple processes beyond diminished cell wall precursor availability; its effect in *C. albicans*' different natural niches and life cycle stages remains to be explored in future experiments.

The metabolomics findings suggested a simple model, by which lack of monomeric precursors for cell wall polysaccharides deprives the cognate enzymes of their substrates, slowing the reaction velocity and leading to decreased structural cell wall polysaccharides and hence decreased cell wall stability (Fig. 9). Diminished cell wall carbohydrate content of P_i-starved chemostat-grown *S. cerevisiae* cells was described 4 decades ago, though a mechanism was not proposed (73). Our model predicts that cells lacking Pho84 would be intolerant not just of beta-1,3-glucan synthase inhibition by micafungin (7) but also of genetic or pharmacologic perturbation of beta-1,6-glucan and chitin synthases. The chitin and beta-1,6-glucan contents of cells lacking Pho84 were sharply decreased (Fig. 4). Similarly, wild-type cells starved for P_i were hypersensitive to inhibitors of chitin and beta-1,3-glucan synthesis, nikkomycin and micafungin (Fig. 5), consistent with combinatorial effects between depletion of the enzyme substrate and direct enzyme inhibition.

Growth defects of strains that we constructed in which expression of the genes encoding the major beta-1,6-glucan synthase, *KRE6*, and the single essential chitin synthase, *CHS1*, is repressible from *pMAL2* (Fig. 6 and 7) or *tetO* were in agreement with the results of Munro et al. (55) but differed from the findings of Han et al. (18, 59). In some *kre6/pMAL2-KRE6* strains, we also deleted the minor beta-1,6-glucan synthase-encoding gene, *SKN1*, and observed no further effect on the phenotype under the analyzed conditions. While transcription from the repressible promoters we used cannot be completely abrogated (56), residual transcription is not expected to sharpen a loss-of-function-associated growth defect. We speculate that the stronger defects of our *kre6* conditional mutants, compared to the homozygous deletion mutant of Han et al., may be attributable to residual Kre6 activity in our mutants, which lowered the likelihood of suppressor mutation emergence.

Loss of Pho84 exacerbated the growth defects exhibited by *CHS1*- and *KRE6*-depleted strains, especially when P_i was not in excess in the medium (Fig. 6 and 7). Conversely, maximally loading cells with P_i by prolonged growth in excess P_i during
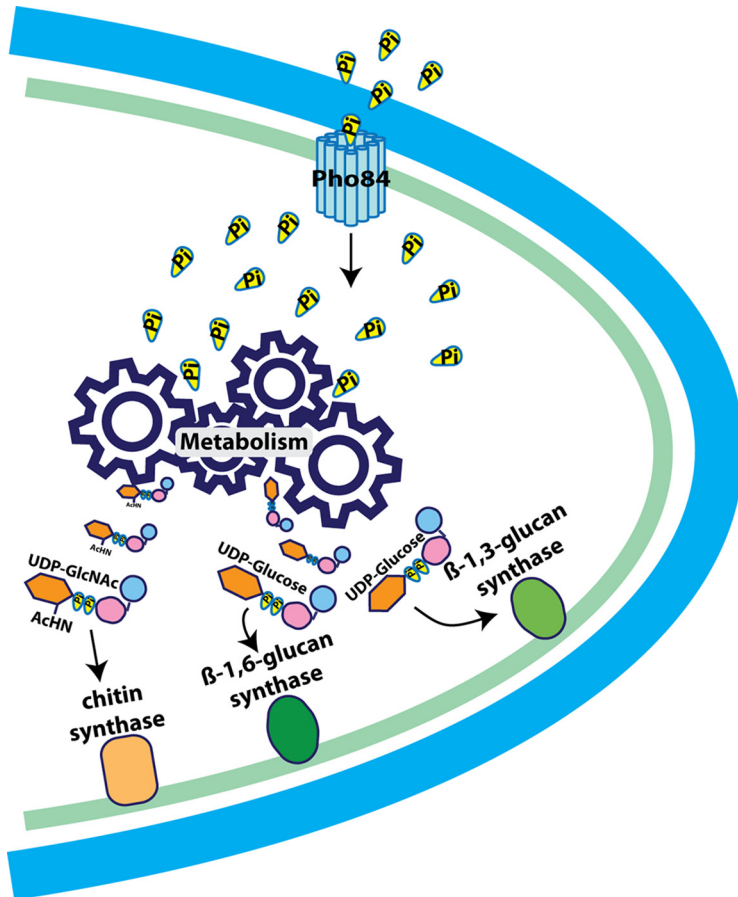
FIG 9 Model: role of Pho84 in cell wall polysaccharide biosynthesis. P_i is imported across the cytoplasmic membrane by Pho84, where it is available to metabolic processes that produce the nucleotide sugars UDP-glucose and UDP-GlcNAc. These nucleotide sugars are the substrates of glucan and chitin synthases that produce major polysaccharides of the cell wall, thereby providing its structural stability.

depletion of the enzyme in question significantly rescued these growth defects (Fig. 6 and 7), supporting the idea that lack of P_i is responsible for synthetic phenotypes of *pho84* with *kre6* or *chs1* mutations.

In agreement with the work of Han et al. (59), we observed a compensatory increase of cell wall chitin (Fig. 8A) in cells depleted of *KRE6*. Han et al. showed that this response depended on intact Mkc1 signaling (59). Absence of Pho84 in *KRE6*-depleted cells abrogated this compensatory response (Fig. 8). Dampened Mkc1 signaling in cells without Pho84 activity (Fig. 1C and Fig. S1) may be one reason for the *pho84*$^{-/-}$ mutants' inability to appropriately upregulate chitin synthase transcription (58, 74). Another reason could be that the concentration of the chitin synthase substrate UDP-GlcNAc was insufficient. The two mechanisms could act together to diminish compensatory chitin synthesis in cells lacking Kre6 as well as Pho84.

Unlike Han et al. (59), we found that very low nikkomycin concentrations further inhibit the growth of *KRE6*-depleted cells, as compensatory chitin synthesis is inhibited (Fig. 8B). This discrepancy could be due to the medium used for assaying the nikkomycin effect: di- and tripeptides, present in YPD but not in the SC medium we used, compete with nikkomycin for uptake into *C. albicans* cells (75, 76). If novel antifungals could be combined to simultaneously inhibit glucan and chitin synthesis, a potent antifungal effect as well as low toxicity in humans, who lack both targets, could be expected.

Induction of high-affinity P_i transporter-encoding genes *PHO84* and *PHO89* in *ex vivo* and *in vivo* models of infection (20–23) shows that during infection, the fungus is

challenged with acquiring P_i, possibly due to alkaline environments in the host (77). While our experimental conditions of prolonged P_i excess are apparently not typical for niches inhabited by *C. albicans*, our results showed that it is limited P_i availability that renders depletion of these cell wall biosynthetic enzymes inhibitory to *C. albicans* growth. They further indicated that during perturbation of biosynthesis of a single cell wall component, P_i availability is limiting for production of compensatory cell wall components like chitin.

Investigators examining *C. albicans* isolates from stool of intensive care unit patients as well as standard laboratory strains hypothesized that phosphate starvation increases hyphal growth and virulence of *C. albicans* (78). Mice that had undergone partial hepatectomy and were drinking tap water, versus a 25 mM phosphate solution, were more susceptible to cecal injection of a *C. albicans* suspension in water than in 25 mM phosphate, respectively, and had more *C. albicans* biofilm on their intestinal mucosa (78). The authors concluded that phosphate starvation had made the *C. albicans* cells more virulent. Mutants in the phosphate starvation response transcriptional regulator Pho4 were considered to produce more hyphae on low-phosphate than on high-phosphate medium and to be more virulent in a *Caenorhabditis elegans* model of infection (78). These findings contrast with those of Ikeh et al., who in multiple *ex vivo* and *in vivo* infection models found null mutants in *PHO4* to be attenuated in virulence (38). Since cells without Pho4 have low levels of Pho84 (38), our results align more closely with those of Ikeh et al. (38), as we found attenuated virulence and defective hyphal growth in cells lacking Pho84 (8). The cell wall integrity defects of *pho84* null mutant cells characterized here may also contribute to their virulence attenuation. Differences in experimental conditions may be responsible for the discrepancies between the results reported by these investigators (78) and await analysis in further experiments.

How limited P_i supplies and essential intermediate metabolites requiring P_i like ATP and phosphoribosyl-pyrophosphate (PRPP) are allocated to different biosynthetic activities of the cell is not known. Decreased phosphomannan, decreased chitin, and decreased beta-1,6-glucan contents suggest that cells lacking P_i prioritize use of this essential element for other metabolic processes. P_i starvation often limits plant growth: P_i-starved oats replace up to 70% of their plasma membrane phospholipids with the glycolipid digalactosyldiacylglycerol (79), a process that is reversible upon P_i refeeding (80). Fungi including the human pathogen *Cryptococcus neoformans* also replace cytoplasmic membrane phospholipids with nonphosphoric lipids during P_i starvation (81, 82). That the cell envelope—the plasma membrane and cell wall—apparently can function while forgoing a share of P_i, while DNA polymerase and ribosomes are absolutely dependent on their P_i allotment, suggests a regulatory mechanism to assign the available P_i to each biosynthetic process. Identification of and interference with this mechanism might lead to a way to disrupt processes required for growth and proliferation of the fungal cell.

Echinocandins and nikkomycin exemplify good tolerability of antifungals whose targets are not conserved in humans (3, 83). Pho84 and beta-1,6-glucan synthases also have no human orthologs. Development and combination of specific small-molecule inhibitors of these targets should potentiate their effects and permit more effective clearance of invasive candidiasis.

MATERIALS AND METHODS

Detailed descriptions of methods are provided in Text S1 in the supplemental material.

Strains and culture conditions. *C. albicans* strains used are shown in Table S2A. Strains were constructed as described in reference 56, using plasmids shown in Table S2B and oligonucleotides shown in Table S2C, using sequences obtained from the Candida Genome Database (84). To minimize phenotypic artifacts originating from genomic events unrelated to the targeted introduced mutations, all genotypes examined were constructed from at least 2 independently engineered heterozygous strains. Experiments with defined ambient P_i concentrations were performed in media based on yeast nitrogen base (YNB) 0 P_i (ForMedium Ltd., Norfolk, United Kingdom) with added KH_2PO_4 to stated concentrations. P_i starvation was induced as described in reference 36. Other media were used as previously indicated (56).

Western blots. Cell lysis and Western blotting were performed as described in reference 30. Antibodies used are listed in Table S2D. At least three biological replicates were obtained.

Alcian blue staining assay. The standard curve and alcian blue binding were determined as in the work of Hobson et al. (34).

Transmission electron microscopy. Each strain was inoculated in standard SC to an optical density at 600 nm (OD_{600}) of 0.1 and grown for 15 h. Cells were then prepared for TEM and analyzed as described in reference 60 with minor modifications.

Intracellular ATP measurement. Cells cultured overnight in YPD medium with a starting OD_{600} of 0.2 were washed with sterile water and lysed. Intracellular ATP levels were measured using the CellTiter-Glo luminescent cell viability assay (Promega; catalog no. G7570), and the results were normalized to the protein concentration. The standard curve was prepared using ATP disodium salt hydrate (Sigma; catalog no. A6419).

Metabolomics. Metabolites were measured as described in reference 39.

Hyphal morphogenesis assay. Cells were resuspended in 0.9% NaCl to an OD_{600} of 0.1. Variations between single colonies as well as colony density effects were minimized by spotting 3-μl cell suspensions at 6 equidistant points, using a template, around the perimeter of an agar medium plate as described in reference 56. Spider medium and RPMI 1640 with glutamine, without sodium bicarbonate (Gibco 31800-022), were used.

Chitin measurement. Cells were grown for 8 h in SC low (0.22 mM) or excess (11 mM) P_i after pregrowth of 3 days' passages in 2× SC-P_i 2% maltose. At the end of pregrowth (time zero) and at 8 h, cells were formaldehyde fixed, washed in phosphate-buffered saline (PBS) before staining with calcofluor white, and then washed extensively in 0.9% NaCl. After sonication, fluorescence intensities of cells were measured by flow cytometry of $\geq 10^5$ events.

***PHO84* promoter induction analysis.** Cells of genotype *PHO84/pPHO84-GFP-NAT1-PHO84* were grown in YPD with additional 10 mM P_i for 16 h and washed three times with 0.9% NaCl, and OD_{600} was adjusted to 0.01 in SC with increasing concentrations of KH_2PO_4. OD_{600} and GFP signal were recorded every 30 min.

Beta-1,6-glucan measurement. Cell wall glucans were extracted, adapting the method of Gilbert et al. (85), by alkali extracting crude cell lysate with 0.75 N NaOH at 75°C for an hour. Supernatants containing alkali-soluble glucans were stored at −80°C until analysis by ELISA. Insoluble pellets were digested with chitinase and Zymolyase in 100 mM K_2HPO_4-KH_2PO_4 buffer (pH 6.0) for 72 h at 37°C followed by 1 h at 45°C. Supernatants of these digests containing alkali-insoluble glucans were stored at −80°C until analysis by ELISA. A competition ELISA using an anti-beta-1,6-glucan antibody (48) was performed with modifications as described in reference 48.

Statistical analysis. Statistical analysis was performed by unpaired Student's *t* test in Prism 7 GraphPad (GraphPad Software, Inc., CA, USA). For metabolomics, MetaboAnalyst (40) was used for analysis including principal-component analysis, heat maps, and pathway analysis.

SUPPLEMENTAL MATERIAL

Supplemental material is available online only.

TEXT S1, PDF file, 0.1 MB.
FIG S1, PDF file, 0.7 MB.
FIG S2, PDF file, 0.3 MB.
FIG S3, PDF file, 0.4 MB.
FIG S4, PDF file, 0.5 MB.
FIG S5, PDF file, 2 MB.
FIG S6, PDF file, 1.8 MB.
TABLE S1, PDF file, 0.1 MB.
TABLE S2, PDF file, 0.1 MB.

REFERENCES

1. Morgan J, Meltzer MI, Plikaytis BD, Sofair AN, Huie-White S, Wilcox S, Harrison LH, Seaberg EC, Hajjeh RA, Teutsch SM. 2005. Excess mortality, hospital stay, and cost due to candidemia: a case-control study using data from population-based candidemia surveillance. Infect Control Hosp Epidemiol 26:540–547. https://doi.org/10.1086/502581.

2. Andes DR, Mycoses Study Group, Safdar N, Baddley JW, Playford G, Reboli AC, Rex JH, Sobel JD, Pappas PG, Kullberg BJ. 2012. Impact of treatment strategy on outcomes in patients with candidemia and other forms of invasive candidiasis: a patient-level quantitative review of randomized trials. Clin Infect Dis 54:1110–1122. https://doi.org/10.1093/cid/cis021.

3. Pappas PG, Kauffman CA, Andes DR, Clancy CJ, Marr KA, Ostrosky-Zeichner L, Reboli AC, Schuster MG, Vazquez JA, Walsh TJ, Zaoutis TE, Sobel JD. 2016. Clinical practice guideline for the management of candidiasis: 2016 update by the Infectious Diseases Society of America. Clin Infect Dis 62:e1–50. https://doi.org/10.1093/cid/civ933.

4. Sawistowska-Schroder ET, Kerridge D, Perry H. 1984. Echinocandin inhibition of 1,3-beta-D-glucan synthase from Candida albicans. FEBS Lett 173:134–138. https://doi.org/10.1016/0014-5793(84)81032-7.

5. Douglas CM. 2001. Fungal beta(1,3)-D-glucan synthesis. Med Mycol 39(Suppl 1):55–66. https://doi.org/10.1080/mmy.39.1.55.66.

6. Munro CA, Whitton RK, Hughes HB, Rella M, Selvaggini S, Gow NA. 2003. CHS8—a fourth chitin synthase gene of Candida albicans contributes to in vitro chitin synthase activity, but is dispensable for growth. Fungal Genet Biol 40:146–158. https://doi.org/10.1016/s1087-1845(03)00083-5.

7. Liu NN, Flanagan PR, Zeng J, Jani NM, Cardenas ME, Moran GP, Köhler JR. 2017. Phosphate is the third nutrient monitored by TOR in Candida albicans and provides a target for fungal-specific indirect TOR inhibition. Proc Natl Acad Sci U S A 114:6346–6351. https://doi.org/10.1073/pnas.1617799114.

8. Liu NN, Uppuluri P, Broggi A, Besold A, Ryman K, Kambara H, Solis N, Lorenz V, Qi W, Acosta Zaldivar M, Emami SN, Bao B, An D, Bonilla F, Sola-Visner M, Filler S, Luo HR, Engstrom Y, Ljungdahl PO, Culotta VC, Zanoni I, Lopez-Ribot JL, Köhler JR. 2018. Intersection of phosphate transport, oxidative stress and TOR signalling in Candida albicans virulence. PLoS Pathog 14:e1007076. https://doi.org/10.1371/journal.ppat.1007076.

9. Hatano K, Morishita Y, Nakai T, Ikeda F. 2002. Antifungal mechanism of FK463 against Candida albicans and Aspergillus fumigatus. J Antibiot (Tokyo) 55:219–222. https://doi.org/10.7164/antibiotics.55.219.

10. Kang MS, Elango N, Mattia E, Au-Young J, Robbins PW, Cabib E. 1984. Isolation of chitin synthetase from Saccharomyces cerevisiae. purification of an enzyme by entrapment in the reaction product. J Biol Chem 259:14966–14972.

11. Au-Young J, Robbins PW. 1990. Isolation of a chitin synthase gene (CHS1) from Candida albicans by expression in Saccharomyces cerevisiae. Mol Microbiol 4:197–207. https://doi.org/10.1111/j.1365-2958.1990.tb00587.x.

12. Gow NA, Robbins PW, Lester JW, Brown AJ, Fonzi WA, Chapman T, Kinsman OS. 1994. A hyphal-specific chitin synthase gene (CHS2) is not essential for growth, dimorphism, or virulence of Candida albicans. Proc Natl Acad Sci U S A 91:6216–6220. https://doi.org/10.1073/pnas.91.13.6216.

13. Mio T, Yabe T, Sudoh M, Satoh Y, Nakajima T, Arisawa M, Yamada-Okabe H. 1996. Role of three chitin synthase genes in the growth of Candida albicans. J Bacteriol 178:2416–2419. https://doi.org/10.1128/jb.178.8.2416-2419.1996.

14. Lenardon MD, Whitton RK, Munro CA, Marshall D, Gow NA. 2007. Individual chitin synthase enzymes synthesize microfibrils of differing structure at specific locations in the Candida albicans cell wall. Mol Microbiol 66:1164–1173. https://doi.org/10.1111/j.1365-2958.2007.05990.x.

15. Roemer T, Delaney S, Bussey H. 1993. SKN1 and KRE6 define a pair of functional homologs encoding putative membrane proteins involved in beta-glucan synthesis. Mol Cell Biol 13:4039–4048. https://doi.org/10.1128/mcb.13.7.4039.

16. Mio T, Yamada-Okabe T, Yabe T, Nakajima T, Arisawa M, Yamada-Okabe H. 1997. Isolation of the Candida albicans homologs of Saccharomyces cerevisiae KRE6 and SKN1: expression and physiological function. J Bacteriol 179:2363–2372. https://doi.org/10.1128/jb.179.7.2363-2372.1997.

17. Vink E, Rodriguez-Suarez RJ, Gérard-Vincent M, Ribas JC, de Nobel H, van den Ende H, Durán A, Klis FM, Bussey H. 2004. An in vitro assay for (1→6)-beta-D-glucan synthesis in Saccharomyces cerevisiae. Yeast 21:1121–1131. https://doi.org/10.1002/yea.1156.

18. Han Q, Wang N, Yao G, Mu C, Wang Y, Sang J. 2019. Blocking beta-1,6-glucan synthesis by deleting KRE6 and SKN1 attenuates the virulence of Candida albicans. Mol Microbiol 111:604–620. https://doi.org/10.1111/mmi.14176.

19. Davis MR, Donnelley MA, Thompson GR. 2019. Ibrexafungerp: a novel oral glucan synthase inhibitor. Med Mycol https://doi.org/10.1093/mmy/myz083.

20. Zakikhany K, Naglik JR, Schmidt-Westhausen A, Holland G, Schaller M, Hube B. 2007. In vivo transcript profiling of Candida albicans identifies a gene essential for interepithelial dissemination. Cell Microbiol 9:2938–2954. https://doi.org/10.1111/j.1462-5822.2007.01009.x.

21. Munoz JF, Delorey T, Ford CB, Li BY, Thompson DA, Rao RP, Cuomo CA. 2019. Coordinated host-pathogen transcriptional dynamics revealed using sorted subpopulations and single macrophages infected with Candida albicans. Nat Commun 10:1607. https://doi.org/10.1038/s41467-019-09599-8.

22. Walker LA, Maccallum DM, Bertram G, Gow NA, Odds FC, Brown AJ. 2009. Genome-wide analysis of Candida albicans gene expression patterns during infection of the mammalian kidney. Fungal Genet Biol 46:210–219. https://doi.org/10.1016/j.fgb.2008.10.012.

23. Hebecker B, Vlaic S, Conrad T, Bauer M, Brunke S, Kapitan M, Linde J, Hube B, Jacobsen ID. 2016. Dual-species transcriptional profiling during systemic candidiasis reveals organ-specific host-pathogen interactions. Sci Rep 6:36055. https://doi.org/10.1038/srep36055.

24. Ram AF, Klis FM. 2006. Identification of fungal cell wall mutants using susceptibility assays based on Calcofluor white and Congo red. Nat Protoc 1:2253–2256. https://doi.org/10.1038/nprot.2006.397.

25. Levin DE. 2011. Regulation of cell wall biogenesis in Saccharomyces cerevisiae: the cell wall integrity signaling pathway. Genetics 189:1145–1175. https://doi.org/10.1534/genetics.111.128264.

26. Heilmann CJ, Sorgo AG, Mohammadi S, Sosinska GJ, de Koster CG, Brul S, de Koning LJ, Klis FM. 2013. Surface stress induces a conserved cell wall stress response in the pathogenic fungus Candida albicans. Eukaryot Cell 12:254–264. https://doi.org/10.1128/EC.00278-12.

27. Navarro-Garcia F, Sanchez M, Pla J, Nombela C. 1995. Functional characterization of the MKC1 gene of Candida albicans, which encodes a mitogen-activated protein kinase homolog related to cell integrity. Mol Cell Biol 15:2197–2206. https://doi.org/10.1128/mcb.15.4.2197.

28. Kumamoto CA. 2005. A contact-activated kinase signals Candida albicans invasive growth and biofilm development. Proc Natl Acad Sci U S A 102:5576–5581. https://doi.org/10.1073/pnas.0407097102.

29. Werner TP, Amrhein N, Freimoser FM. 2005. Novel method for the quantification of inorganic polyphosphate (iPoP) in Saccharomyces cerevisiae shows dependence of iPoP content on the growth phase. Arch Microbiol 184:129–136. https://doi.org/10.1007/s00203-005-0031-2.

30. Chowdhury T, Köhler JR. 2015. Ribosomal protein S6 phosphorylation is controlled by TOR and modulated by PKA in Candida albicans. Mol Microbiol 98:384–402. https://doi.org/10.1111/mmi.13130.

31. Nishikawa A, Poster JB, Jigami Y, Dean N. 2002. Molecular and phenotypic analysis of CaVRG4, encoding an essential Golgi apparatus GDP-mannose transporter. J Bacteriol 184:29–42. https://doi.org/10.1128/jb.184.1.29-42.2002.

32. Walker L, Sood P, Lenardon MD, Milne G, Olson J, Jensen G, Wolf J, Casadevall A, Adler-Moore J, Gow N. 2018. The viscoelastic properties of the fungal cell wall allow traffic of ambisome as intact liposome vesicles. mBio 9:e02383-17. https://doi.org/10.1128/mBio.02383-17.

33. Karson EM, Ballou CE. 1978. Biosynthesis of yeast mannan. Properties of a mannosylphosphate transferase in Saccharomyces cerevisiae. J Biol Chem 253:6484–6492.

34. Hobson RP, Munro CA, Bates S, MacCallum DM, Cutler JE, Heinsbroek SE, Brown GD, Odds FC, Gow NA. 2004. Loss of cell wall mannosylphosphate in Candida albicans does not influence macrophage recognition. J Biol Chem 279:39628–39635. https://doi.org/10.1074/jbc.M405003200.

35. Konopka JB. 2012. N-acetylglucosamine (GlcNAc) functions in cell signaling. Scientifica (Cairo) 2012:489208. https://doi.org/10.6064/2012/489208.

36. Popova Y, Thayumanavan P, Lonati E, Agrochao M, Thevelein JM. 2010. Transport and signaling through the phosphate-binding site of the yeast

Pho84 phosphate transceptor. Proc Natl Acad Sci U S A 107:2890–2895. https://doi.org/10.1073/pnas.0906546107.

37. Thomas MR, O'Shea EK. 2005. An intracellular phosphate buffer filters transient fluctuations in extracellular phosphate levels. Proc Natl Acad Sci U S A 102:9565–9570. https://doi.org/10.1073/pnas.0501122102.

38. Ikeh MA, Kastora SL, Day AM, Herrero-de-Dios CM, Tarrant E, Waldron KJ, Banks AP, Bain JM, Lydall D, Veal EA, MacCallum DM, Erwig LP, Brown AJ, Quinn J. 2016. Pho4 mediates phosphate acquisition in Candida albicans and is vital for stress resistance and metal homeostasis. Mol Biol Cell 27:2784–2801. https://doi.org/10.1091/mbc.E16-05-0266.

39. Yuan M, Breitkopf SB, Yang X, Asara JM. 2012. A positive/negative ion-switching, targeted mass spectrometry-based metabolomics platform for bodily fluids, cells, and fresh and fixed tissue. Nat Protoc 7:872–881. https://doi.org/10.1038/nprot.2012.024.

40. Xia J, Wishart DS. 2011. Web-based inference of biological patterns, functions and pathways from metabolomic data using MetaboAnalyst. Nat Protoc 6:743–760. https://doi.org/10.1038/nprot.2011.319.

41. Grahl N, Demers EG, Lindsay AK, Harty CE, Willger SD, Piispanen AE, Hogan DA. 2015. Mitochondrial activity and Cyr1 are key regulators of Ras1 activation of C. albicans virulence pathways. PLoS Pathog 11:e1005133. https://doi.org/10.1371/journal.ppat.1005133.

42. Azevedo C, Saiardi A. 2017. Eukaryotic phosphate homeostasis: the inositol pyrophosphate perspective. Trends Biochem Sci 42:219–231. https://doi.org/10.1016/j.tibs.2016.10.008.

43. Esher SK, Ost KS, Kohlbrenner MA, Pianalto KM, Telzrow CL, Campuzano A, Nichols CB, Munro C, Wormley FL, Jr, Alspaugh JA. 2018. Defects in intracellular trafficking of fungal cell wall synthases lead to aberrant host immune recognition. PLoS Pathog 14:e1007126. https://doi.org/10.1371/journal.ppat.1007126.

44. Kim MK, Park HS, Kim CH, Park HM, Choi W. 2002. Inhibitory effect of nikkomycin Z on chitin synthases in Candida albicans. Yeast 19:341–349. https://doi.org/10.1002/yea.837.

45. Shubitz LF, Trinh HT, Perrill RH, Thompson CM, Hanan NJ, Galgiani JN, Nix DE. 2014. Modeling nikkomycin Z dosing and pharmacology in murine pulmonary coccidioidomycosis preparatory to phase 2 clinical trials. J Infect Dis 209:1949–1954. https://doi.org/10.1093/infdis/jiu029.

46. Kollar R, Reinhold BB, Petrakova E, Yeh HJ, Ashwell G, Drgonova J, Kapteyn JC, Klis FM, Cabib E. 1997. Architecture of the yeast cell wall. Beta(1→6)-glucan interconnects mannoprotein, beta(1→3)-glucan, and chitin. J Biol Chem 272:17762–17775. https://doi.org/10.1074/jbc.272.28.17762.

47. Roemer T, Bussey H. 1991. Yeast beta-glucan synthesis: KRE6 encodes a predicted type II membrane protein required for glucan synthesis in vivo and for glucan synthase activity in vitro. Proc Natl Acad Sci U S A 88:11295–11299. https://doi.org/10.1073/pnas.88.24.11295.

48. Kottom TJ, Hebrink DM, Jenson PE, Gudmundsson G, Limper AH. 2015. Evidence for proinflammatory beta-1,6 glucans in the Pneumocystis carinii cell wall. Infect Immun 83:2816–2826. https://doi.org/10.1128/IAI.00196-15.

49. Sietsma JH, Wessels JGH. 1979. Evidence for covalent linkages between chitin and beta-glucan in a fungal wall. J Gen Microbiol 114:99–108. https://doi.org/10.1099/00221287-114-1-99.

50. Sietsma JH, Wessels JG. 1981. Solubility of (1→3)-beta-D/(1→6)-beta-D-glucan in fungal walls: importance of presumed linkage between glucan and chitin. J Gen Microbiol 125:209–212. https://doi.org/10.1099/00221287-125-1-209.

51. Fontaine T, Simenel C, Dubreucq G, Adam O, Delepierre M, Lemoine J, Vorgias CE, Diaquin M, Latge JP. 2000. Molecular organization of the alkali-insoluble fraction of Aspergillus fumigatus cell wall. J Biol Chem 275:27594–27607. https://doi.org/10.1074/jbc.M909975199.

52. Kollar R, Petrakova E, Ashwell G, Robbins PW, Cabib E. 1995. Architecture of the yeast cell wall. The linkage between chitin and beta(1→3)-glucan. J Biol Chem 270:1170–1178. https://doi.org/10.1074/jbc.270.3.1170.

53. Sullivan PA, Yin CY, Molloy C, Templeton MD, Shepherd MG. 1983. An analysis of the metabolism and cell wall composition of Candida albicans during germ-tube formation. Can J Microbiol 29:1514–1525. https://doi.org/10.1139/m83-233.

54. Kitamura A, Higuchi S, Hata M, Kawakami K, Yoshida K, Namba K, Nakajima R. 2009. Effect of beta-1,6-glucan inhibitors on the invasion process of Candida albicans: potential mechanism of their in vivo efficacy. Antimicrob Agents Chemother 53:3963–3971. https://doi.org/10.1128/AAC.00435-09.

55. Munro CA, Winter K, Buchan A, Henry K, Becker JM, Brown AJ, Bulawa CE, Gow NA. 2001. Chs1 of Candida albicans is an essential chitin synthase required for synthesis of the septum and for cell integrity. Mol Microbiol 39:1414–1426. https://doi.org/10.1046/j.1365-2958.2001.02347.x.

56. Shen J, Cowen LE, Griffin AM, Chan L, Köhler JR. 2008. The Candida albicans pescadillo homolog is required for normal hypha-to-yeast morphogenesis and yeast proliferation. Proc Natl Acad Sci U S A 105:20918–20923. https://doi.org/10.1073/pnas.0809147105.

57. Walker LA, Munro CA, de Bruijn I, Lenardon MD, McKinnon A, Gow NA. 2008. Stimulation of chitin synthesis rescues Candida albicans from echinocandins. PLoS Pathog 4:e1000040. https://doi.org/10.1371/journal.ppat.1000040.

58. Lenardon MD, Lesiak I, Munro CA, Gow NA. 2009. Dissection of the Candida albicans class I chitin synthase promoters. Mol Genet Genomics 281:459–471. https://doi.org/10.1007/s00438-009-0423-0.

59. Han Q, Wang N, Pan C, Wang Y, Sang J. 2019. Elevation of cell wall chitin via Ca²⁺-calcineurin-mediated PKC signaling pathway maintains the viability of Candida albicans in the absence of beta-1,6-glucan synthesis. Mol Microbiol 112:960–972. https://doi.org/10.1111/mmi.14335.

60. Hall RA, Bates S, Lenardon MD, Maccallum DM, Wagener J, Lowman DW, Kruppa MD, Williams DL, Odds FC, Brown AJ, Gow NA. 2013. The Mnn2 mannosyltransferase family modulates mannoprotein fibril length, immune recognition and virulence of Candida albicans. PLoS Pathog 9:e1003276. https://doi.org/10.1371/journal.ppat.1003276.

61. Köhler JR, Fink GR. 1996. Candida albicans strains heterozygous and homozygous for mutations in mitogen-activated protein kinase signaling components have defects in hyphal development. Proc Natl Acad Sci U S A 93:13223–13228. https://doi.org/10.1073/pnas.93.23.13223.

62. Uhl MA, Biery M, Craig N, Johnson AD. 2003. Haploinsufficiency-based large-scale forward genetic analysis of filamentous growth in the diploid human fungal pathogen C.albicans. EMBO J 22:2668–2678. https://doi.org/10.1093/emboj/cdg256.

63. Boer VM, Crutchfield CA, Bradley PH, Botstein D, Rabinowitz JD. 2010. Growth-limiting intracellular metabolites in yeast growing under diverse nutrient limitations. Mol Biol Cell 21:198–211. https://doi.org/10.1091/mbc.e09-07-0597.

64. Machado CM, De-Souza EA, De-Queiroz ALFV, Pimentel FSA, Silva GFS, Gomes FM, Montero-Lomelí M, Masuda CA. 2017. The galactose-induced decrease in phosphate levels leads to toxicity in yeast models of galactosemia. Biochim Biophys Acta Mol Basis Dis 1863:1403–1409. https://doi.org/10.1016/j.bbadis.2017.02.014.

65. Gibney PA, Schieler A, Chen JC, Bacha-Hummel JM, Botstein M, Volpe M, Silverman SJ, Xu Y, Bennett BD, Rabinowitz JD, Botstein D. 2018. Common and divergent features of galactose-1-phosphate and fructose-1-phosphate toxicity in yeast. Mol Biol Cell 29:897–910. https://doi.org/10.1091/mbc.E17-11-0666.

66. Nelson DL, Cox MM. 2017. Principles of biochemistry, 7th ed. Macmillan Learning, New York, NY.

67. Chamilos G, Lewis RE, Kontoyiannis DP. 2006. Inhibition of Candida parapsilosis mitochondrial respiratory pathways enhances susceptibility to caspofungin. Antimicrob Agents Chemother 50:744–747. https://doi.org/10.1128/AAC.50.2.744-747.2006.

68. Chen YL, Montedonico AE, Kauffman S, Dunlap JR, Menn FM, Reynolds TB. 2010. Phosphatidylserine synthase and phosphatidylserine decarboxylase are essential for cell wall integrity and virulence in Candida albicans. Mol Microbiol 75:1112–1132. https://doi.org/10.1111/j.1365-2958.2009.07018.x.

69. Dagley MJ, Gentle IE, Beilharz TH, Pettolino FA, Djordjevic JT, Lo TL, Uwamahoro N, Rupasinghe T, Tull DL, McConville M, Beaurepaire C, Nantel A, Lithgow T, Mitchell AP, Traven A. 2011. Cell wall integrity is linked to mitochondria and phospholipid homeostasis in Candida albicans through the activity of the post-transcriptional regulator Ccr4-Pop2. Mol Microbiol 79:968–989. https://doi.org/10.1111/j.1365-2958.2010.07503.x.

70. Qu Y, Jelicic B, Pettolino F, Perry A, Lo TL, Hewitt VL, Bantun F, Beilharz TH, Peleg AY, Lithgow T, Djordjevic JT, Traven A. 2012. Mitochondrial sorting and assembly machinery subunit Sam37 in Candida albicans: insight into the roles of mitochondria in fitness, cell wall integrity, and virulence. Eukaryot Cell 11:532–544. https://doi.org/10.1128/EC.05292-11.

71. She X, Calderone R, Kruppa M, Lowman D, Williams D, Zhang L, Gao Y, Khamooshi K, Liu W, Li D. 2016. Cell wall N-linked mannoprotein biosynthesis requires Goa1p, a putative regulator of mitochondrial complex I in Candida albicans. PLoS One 11:e0147175. https://doi.org/10.1371/journal.pone.0147175.

72. Duvenage L, Walker LA, Bojarczuk A, Johnston SA, MacCallum DM, Munro CA, Gourlay CW. 2019. Inhibition of classical and alternative

modes of respiration in Candida albicans leads to cell wall remodeling and increased macrophage recognition. mBio 10:e02535-18. https://doi .org/10.1128/mBio.02535-18.

73. Ramsay AM, Douglas LJ. 1979. Effects of phosphate limitation of growth on the cell-wall and lipid composition of Saccharomyces cerevisiae. J Gen Microbiol 110:185–191. https://doi.org/10.1099/00221287-110-1-185.

74. Munro CA, Selvaggini S, de Bruijn I, Walker L, Lenardon MD, Gerssen B, Milne S, Brown AJ, Gow NA. 2007. The PKC, HOG and Ca2+ signalling pathways co-ordinately regulate chitin synthesis in Candida albicans. Mol Microbiol 63:1399–1413. https://doi.org/10.1111/j.1365-2958.2007 .05588.x.

75. Yadan JC, Gonneau M, Sarthou P, Le Goffic F. 1984. Sensitivity to nikkomycin Z in Candida albicans: role of peptide permeases. J Bacteriol 160:884–888. https://doi.org/10.1128/JB.160.3.884-888.1984.

76. McCarthy PJ, Troke PF, Gull K. 1985. Mechanism of action of nikkomycin and the peptide transport system of Candida albicans. J Gen Microbiol 131:775–780. https://doi.org/10.1099/00221287-131-4-775.

77. Lev S, Djordjevic JT. 2018. Why is a functional PHO pathway required by fungal pathogens to disseminate within a phosphate-rich host: a paradox explained by alkaline pH-simulated nutrient deprivation and expanded PHO pathway function. PLoS Pathog 14:e1007021. https://doi .org/10.1371/journal.ppat.1007021.

78. Romanowski K, Zaborin A, Valuckaite V, Rolfes RJ, Babrowski T, Bethel C, Olivas A, Zaborina O, Alverdy JC. 2012. Candida albicans isolates from the gut of critically ill patients respond to phosphate limitation by expressing filaments and a lethal phenotype. PLoS One 7:e30119. https://doi.org/10.1371/journal.pone.0030119.

79. Andersson MX, Stridh MH, Larsson KE, Liljenberg C, Sandelius AS. 2003. Phosphate-deficient oat replaces a major portion of the plasma membrane phospholipids with the galactolipid digalactosyldiacylglycerol. FEBS Lett 537:128–132. https://doi.org/10.1016/S0014-5793(03)00109-1.

80. Tjellstrom H, Andersson MX, Larsson KE, Sandelius AS. 2008. Membrane phospholipids as a phosphate reserve: the dynamic nature of phospholipid-to-digalactosyl diacylglycerol exchange in higher plants. Plant Cell Environ 31:1388–1398. https://doi.org/10.1111/j.1365-3040 .2008.01851.x.

81. Riekhof WR, Naik S, Bertrand H, Benning C, Voelker DR. 2014. Phosphate starvation in fungi induces the replacement of phosphatidylcholine with the phosphorus-free betaine lipid diacylglyceryl-N,N,N-trimethylhomoserine. Eukaryot Cell 13:749–757. https://doi.org/10.1128/ EC.00004-14.

82. Lev S, Rupasinghe T, Desmarini D, Kaufman-Francis K, Sorrell TC, Roessner U, Djordjevic JT. 2019. The PHO signaling pathway directs lipid remodeling in Cryptococcus neoformans via DGTS synthase to recycle phosphate during phosphate deficiency. PLoS One 14:e0212651. https:// doi.org/10.1371/journal.pone.0212651.

83. Van Dyke MCC, Thompson GR, Galgiani JN, Barker BM. 2019. The rse of Coccidioides: forces against the dust devil unleashed. Front Immunol 10:2188. https://doi.org/10.3389/fimmu.2019.02188.

84. Skrzypek MS, Binkley J, Binkley G, Miyasato SR, Simison M, Sherlock G. 2017. The Candida Genome Database (CGD): incorporation of Assembly 22, systematic identifiers and visualization of high throughput sequencing data. Nucleic Acids Res 45:D592–D596. https://doi.org/10.1093/nar/ gkw924.

85. Gilbert NM, Donlin MJ, Gerik KJ, Specht CA, Djordjevic JT, Wilson CF, Sorrell TC, Lodge JK. 2010. KRE genes are required for beta-1,6-glucan synthesis, maintenance of capsule architecture and cell wall protein anchoring in Cryptococcus neoformans. Mol Microbiol 76:517–534. https://doi.org/10.1111/j.1365-2958.2010.07119.x.